Journal of Organometallic Chemistry 695 (2010) 1253–1260

Contents lists available at ScienceDirect

Journal of Organometallic Chemistry

journal homepage: www.elsevier.com/locate/jorganchem

Note

Stepwise phosphine sulfide formation and metal-bridging reaction of tetradentate and tridentate phosphine ligands on palladium(II)

Sen-ichi Aizawa [a,*], Tatsuya Kawamoto [b], Yuuto Asai [a], Chie Ishimura [a]

[a] Graduate School of Science and Engineering, University of Toyama, 3190 Gofuku, Toyama 930-8555, Japan
[b] Department of Chemistry, Faculty of Science, Kanagawa University, Hiratsuka, Kanagawa 259-1293, Japan

ARTICLE INFO

Article history:
Received 1 December 2009
Received in revised form 1 February 2010
Accepted 5 February 2010
Available online 12 February 2010

Keywords:
Kinetics
Phosphine sulfide formation
Phosphine-bridging reaction
Steric conversion mechanism

ABSTRACT

Kinetic studies on the stepwise phosphine sulfide formation reaction of the five-coordinate trigonal-bipyramidal Pd(II) complexes with the tripodal tetradentate phosphine ligand, $[PdCl(pp_3)]Cl$ and $[Pd(4\text{-}Cltp)(pp_3)](BF_4)$ (pp_3 = tris[2-(diphenylphosphino)ethyl]phosphine; 4-Cltp = 4-chlorothiophenolate), were carried out, and it was revealed that the reactions proceeded via the intermediate with a pendant dissociated phosphino group. Formation of the intermediate was utilized for the bridging reaction onto Pt(II) to form the phosphine-bridged linear trinuclear and cyclic tetranuclear mixed-metal complexes. Difference in the steric conversion mechanism in the phosphine-bridging reaction between the linear tridentate phosphine (bis[2-(diphenylphosphino)ethyl]phenylphosphine) and pp_3 is also reported.

1. Introduction

Some phosphine sulfides have been employed as monodentate or bidentate ligands for some metal ions [1–6], and we have applied multidentate phosphine sulfide ligands to the Pd(0) catalyzed C–C coupling reaction to stabilize the zerovalent oxidation state of palladium [7]. However, so far, kinetic study on phosphine sulfide formation reactions of phosphine complexes has not been reported.

Recently, we have found that two phosphine chalcogenide groups are selectively formed on the five-coordinate trigonal-bipyramidal Pd(II) complex with tripodal tetradentate phosphine, tris[2-(diphenylphosphino)ethyl]phosphine (pp_3), by the reaction with excess sulfur or selenium [8], and we have also reported the stepwise phosphine-bridging reaction to give the trinuclear and pentanuclear mixed-metal complexes with intended metal sequences quantitatively [9]. We have assumed that such success in selective preparations is attributed to formation of the Pd(II) intermediate with a pendant dissociated phosphino group. In order to confirm the reaction mechanism of the phosphine chalcogenide formation and phosphine-bridging reaction, we have carried out kinetic studies on the phosphine sulfide formation reaction of the Pd(II) complexes with pp_3 considering that sulfur, which has moderately high solubility in nonpolar solvents, is suitable reactant for kinetic experiments. Furthermore, we have compared the phosphine-bridging reaction of the square-planar Pd(II) complex with bis[2-(diphenylphosphino)ethyl]phenylphosphine (p_3) to that of the trigonal-bipyramidal complex with pp_3. As a result, we have found interesting difference in the isomerization mechanism of the phosphine-bridged polynuclear complex between the p_3 and pp_3 ligand systems.

2. Experimental

2.1. Reagents

Chloroform (Wako, ∞ pure) for kinetic measurements were dried over activated 4A Molecular Sieves. Tris[2-(diphenylphosphino)ethyl]phosphine (pp_3, Aldrich), bis[2-(diphenylphosphino)-ethyl]phenylphosphine (p_3, Aldrich), sulfur (Wako), tetrakis(acetonitrile)palladium(II) tetrafluoroborate ($[Pd(CH_3CN)_4](BF_4)_2$, Aldrich), tetra(*n*-butyl)ammonium chloride (Bu_4NCl, Wako), potassium tetrachloropalladate(II) ($K_2[PdCl_4]$, Aldrich), potassium tetrachloroplatinate (II) ($K_2[PtCl_4]$, Aldrich), *cis*- and *trans*-bis(benzonitrile)dichloroplatinum(II) (*cis*- and *trans*-$[PtCl_2(NCC_6H_5)_2]$, Aldrich and Strem, respectively), nickel chloride (Wako), and 4-chlorothiophenol (H-4-Cltp, Wako) were used without further purification.

2.2. Preparation

The mononuclear phosphine complexes $[PdCl(pp_3)]Cl$ (**1**) [10], $[PdCl(pp_3)](BF_4)$ (**2**) [9], $[Pd(4\text{-}Cltp)(pp_3)](BF_4)$ (**3**) [11], $[PdCl(p_3)]Cl$

* Corresponding author. Tel./fax: +81 76 445 6980.
E-mail address: saizawa@eng.u-toyama.ac.jp (S.-i. Aizawa).

0022-328X/$ - see front matter © 2010 Elsevier B.V. All rights reserved.
doi:10.1016/j.jorganchem.2010.02.006

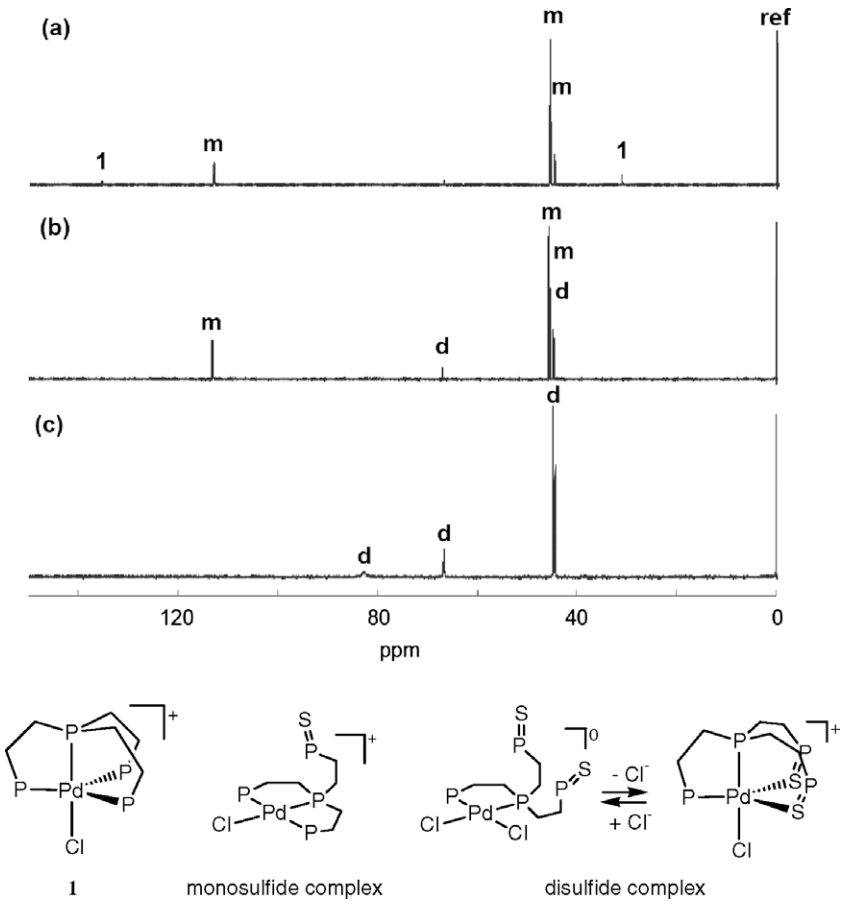

Fig. 1. ^{31}P NMR spectral change of a chloroform solution containing **1** (27 mmol kg^{-1}) and sulfur (420 mmol kg^{-1}) at room temperature. The spectra were recorded at 15 min (a) and 75 min (b) after the reaction was started and after the reaction was completed (c), respectively. m and d denote the monosulfide and disulfide complexes, respectively.

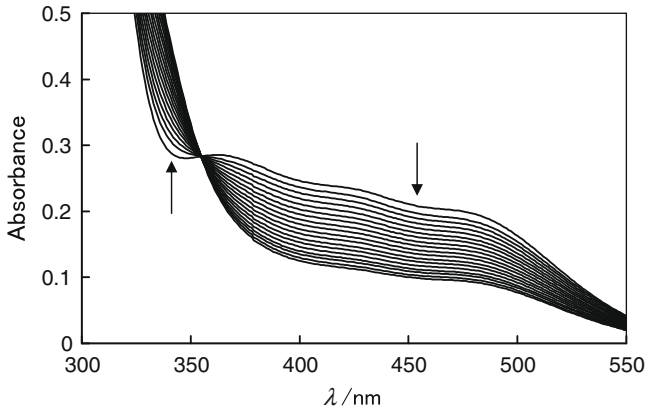

Fig. 2. Absorption spectral change of a chloroform solution containing **1** (0.08 mmol kg^{-1}) and sulfur (1.6 mmol kg^{-1}) at 313.15 K. The spectra were recorded at 0.5, 10, 20, 30, 40, 50, 60, 70, 80, 90, 100, 110, 120, 130, 140, 150, 160, and 170 min after the temperature was equilibrated. The directions of the spectral change are denoted by arrows.

(**4**) [10], [PtCl(pp$_3$)]Cl (**5**) [12], and [NiCl(pp$_3$)]Cl (**6**) [9] were prepared by the reported procedures.

The trinuclear phosphine-bridged complex *trans*-[PtCl$_2${PdCl$_2$-(p$_3$)}$_2$] was prepared by the reaction of **4** (0.15 g, 0.16 mmol) with *cis*-[PtCl$_2$(NCC$_6$H$_5$)$_2$] (0.038 g, 0.080 mmol) in chloroform (5 cm^3). The reaction solution was concentrated with a rotary evaporator and to this was added diethyl ether. The mixture was kept in a refrigerator to give yellow single crystals for an X-ray analysis.

Table 1
Activation parameters for phosphine sulfide formation reactions of **1** and **3**.

Complex	Reaction	k (mol^{-1} kg s^{-1})	$\Delta H^{\ddagger}$ (kJ mol^{-1})	$\Delta S^{\ddagger}$ (J K^{-1} mol^{-1})
1	First step	9.8×10^{-3}	51.2 ± 1.0	−112 ± 3
	Second step	2.1×10^{-2}	54.0 ± 2.1	−96 ± 7
3	First step	2.9×10^{-2}	55.2 ± 2.0	−89 ± 7
	Second step	6.8×10^{-5} [a]	65.5 ± 2.9	−105 ± 9

[a] Unit is s^{-1}.

2.3. Crystal structure determination

X-ray crystallographic data for *trans*-[PtCl$_2${PdCl$_2$(p$_3$)}$_2$] were collected with the ω scan technique on a Rigaku RAXIS-RAPID image plate diffractometer with graphite monochromated Mo Kα (λ = 0.71075 Å) radiation at 200 K. Empirical absorption corrections were applied. The structure was solved and refined using the SHELXS-97 [13] and SHELXL-97 [14] software. All non-hydrogen atoms

were refined anisotropically and hydrogen atoms were included in calculated positions.

2.4. Measurements

The kinetic measurements for the formation reactions of the phosphine sulfide complexes in chloroform were performed at 288–333 K under pseudo-first-order conditions where the concentrations of sulfur were in large excess (1.5×10^{-3}–3.75×10^{-2} mol kg^{-1} for **1** and 7.5×10^{-3}–6.0×10^{-2} mol kg^{-1} for **2**) over those of **1** (7.5×10^{-5} mol kg^{-1}) and **2** (1.5×10^{-4} mol kg^{-1}). The temperature of the reaction solution was controlled within ±0.1 K. The absorption spectral changes were recorded on a Perkin–Elmer Lambda 19 spectrophotometer.

^{31}P NMR spectra were recorded on a JEOL JNM-A400 FT-NMR spectrometer operating at 160.70 MHz. In order to determine the chemical shifts of ^{31}P NMR signals, a 3 mm o.d. NMR tube containing the sample solution was coaxially mounted in a 5 mm o.d. NMR tube containing deuterated water as a lock solvent and phosphoric acid as a reference.

3. Results and discussion

3.1. Kinetics

Previously, we reported the formation of the monosulfide and disulfide complexes by the reactions of **1** with 1 equiv. and excess sulfur, respectively [8]. As shown in Fig. 1, the sulfide complex formation with excess sulfur was stepwise. The first step showed the formation of the square-planar monosulfide complex with a pendant phosphine sulfide group and coordinated two terminal and one central phosphino groups, and the second step gave three coalesced signals of the disulfide complex that exists in a rapid equilibrium between the square-planar complex with two pendant phosphine sulfide groups and the five-coordinate complex with two coordinated phosphine sulfide groups as reported [8]. The complex **1** exhibits three absorption bands in the visible region, and the first and second step correspond to disappearance of the absorption at the shortest wavelength (ca. 370 nm) and subsequent decrease of the other two absorption bands, respectively (Fig. 2). The rate constants for the monosulfide formation were obtained by the initial slope method following change in the absorbance at 425 nm, and the rate constants for the disulfide formation were obtained by a nonlinear least-square analysis for the exponential time course of the absorbance at 450 nm after complete disappearance of the absorption at ca. 370 nm. The observed rate constants (k_{obs}) for both sulfide formation steps are first-order with respect to the sulfur concentration (Figs. S1 and S2). Temperature

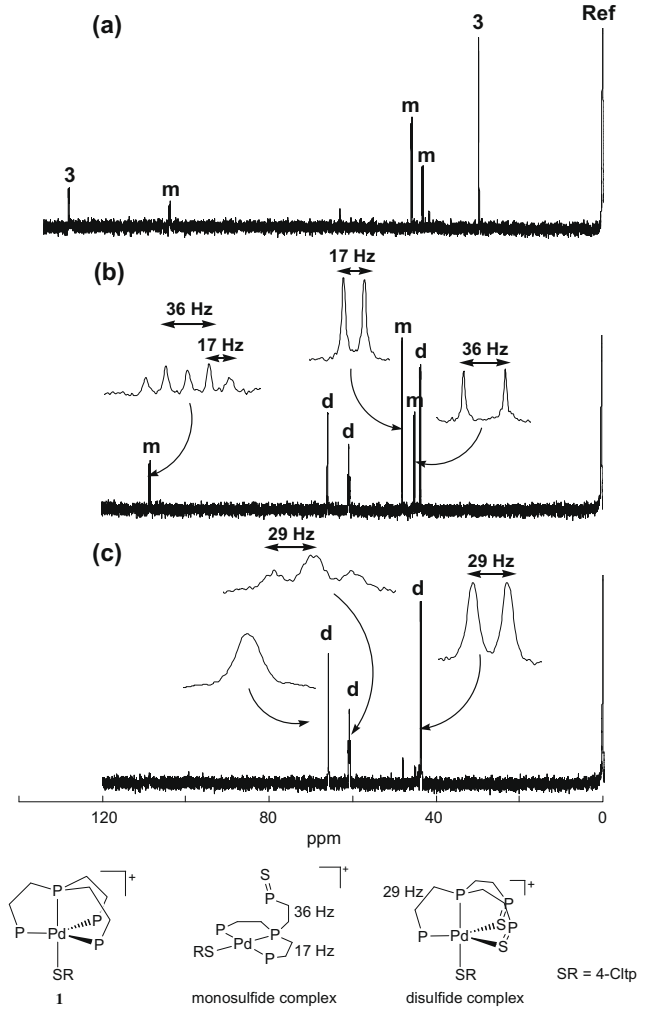

Fig. 3. ^{31}P NMR spectral change of a chloroform solution containing **3** (8.6 mmol kg^{-1}) and sulfur (37 mmol kg^{-1}) at room temperature. The spectra were recorded at 15 min (a) and 2 h (b) after the reaction was started and after the reaction was completed (c), respectively. m and d denote the monosulfide and disulfide complexes, respectively.

dependences of the second-order rate constants were fitted to the Eyring equation (Fig. S3) to give the activation enthalpies ($\Delta H^{\ddagger}$) and activation entropies ($\Delta S^{\ddagger}$) (Table 1). The first-order sulfur concentration dependence of k_{obs} and the large negative values of $\Delta S^{\ddagger}$ suggest the associative sulfide formation with pre-dissociation of the coordinated phosphino groups (Scheme 1). In the case of

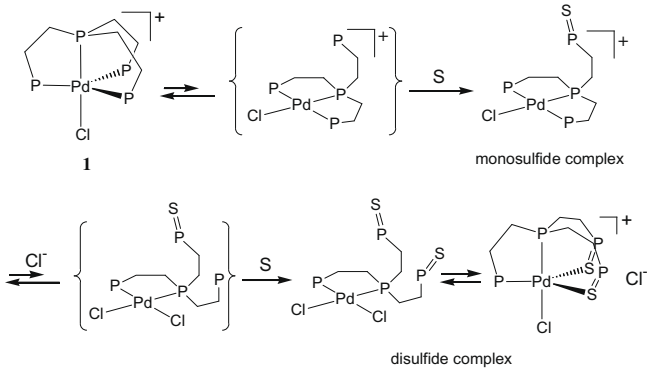

Scheme 1.

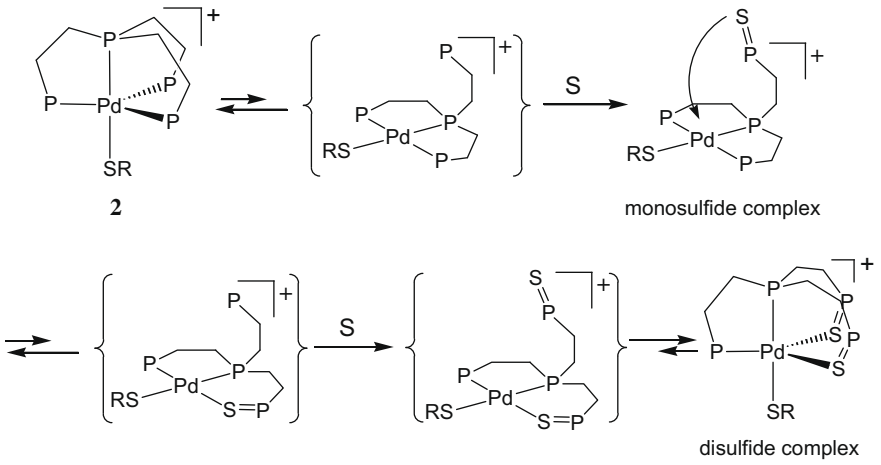

Scheme 2.

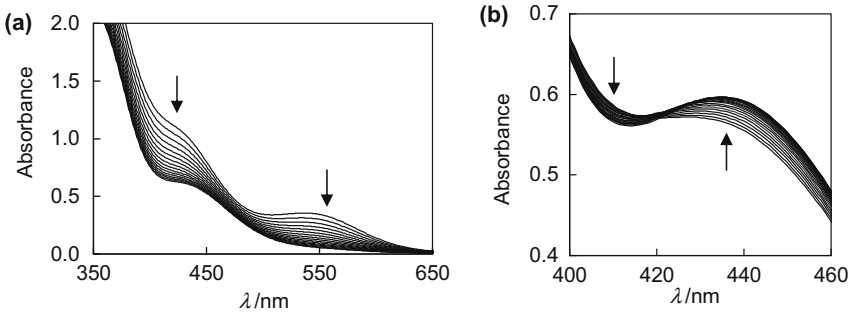

Fig. 4. Absorption spectral change of a chloroform solution containing **3** (0.15 mmol kg^{-1}) and sulfur (14.7 mmol kg^{-1}) at 298.15 K. The spectra were recorded at 0, 5, 10, 15, 20, 25, 30, 35, 40, 45, 50, 55, 60, 65, 70, and 75 min (a) and at 180, 195, 210, 225, 240, 255, 270, 285, 300, 315, 330, 345, 360, 375, 390, 405, 420, 435, 450, 465, and 480 min (b) after the temperature was equilibrated. The directions of the spectral changes are denoted by arrows.

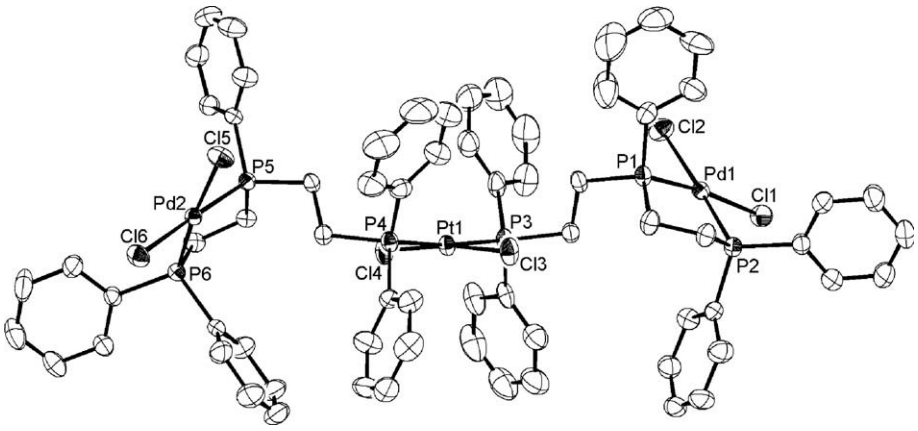

Fig. 5. ORTEP diagram of *trans*-[$PtCl_2\{PdCl_2(p_3)\}_2$].

2 having BF_4^- counter ion instead of Cl^-, the disulfide complex was not formed to give only the monosulfide one even though excess sulfur was used. This fact indicates that coordination of a chloride ion is necessary for the pre-dissociation of the coordinated phosphino group in the second step (Scheme 1).

In contrast with the chloro complex **2**, the thiolato complex **3**, which has also BF_4^- as a counter anion, gave the disulfide complex by the reaction with excess sulfur. The ^{31}P NMR spectra in Fig. 3 shows the formation of the square-planar monosulfide complex similar to the first step for **1** and **2** followed by the formation of

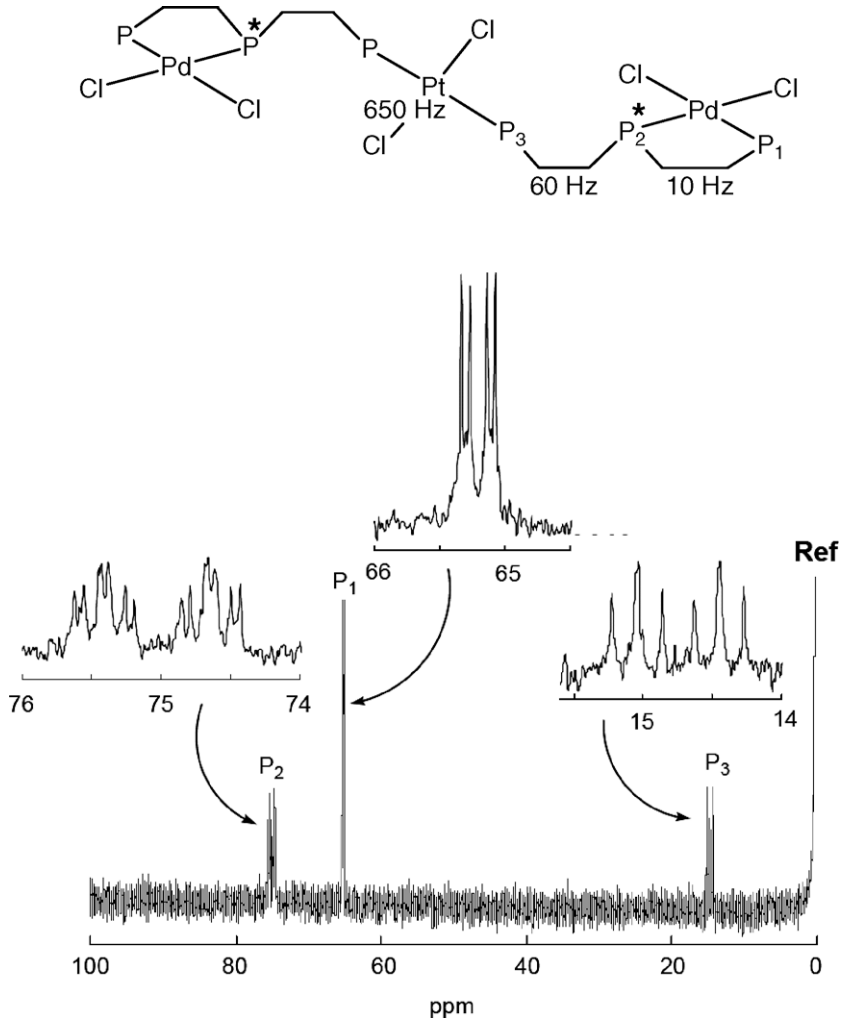

Fig. 6. ^{31}P NMR spectrum of *trans*-[$PtCl_2\{PdCl_2(p_3)\}_2$] in chloroform.

the five-coordinate disulfide complex without any equilibrium for the second step. Considering that BF_4^- does not participate in the substitution reaction as shown in the reaction of **2**, it is apparent that the second step proceeds with the intramolecular substitution of the coordinated phosphino group for the pendant phosphine sulfide group in the square-planar monosulfide complex (Scheme 2). The sulfur–phosphorus π bonding orbital is not so stabilized, and consequently the unoccupied π^* orbital is moderately low and can be a good π-accepting orbital for the metal center [15]. Since the thiolato sulfur atom in **3** is a strong σ and π donor compared with chloride ion, it is reasonable to assume that π-accepting P═S coordination is stabilized in the intermediate for **3** compared with **1**. As shown in Fig. 4, the first and second steps correspond to decrease in absorbance in the visible region (Fig. 4a) and subsequent increase in absorbance in the wavelength region longer than 422 nm, at which the isosbestic point is observed (Fig. 4b), respectively. The rate constants for the monosulfide and disulfide formations were obtained by nonlinear least-square analyzes for the exponential time courses of the absorbances at 540 and 450 nm, respectively. While k_{obs} for the monosulfide formation is proportional to the excess sulfur concentration (Fig. S4), k_{obs} for the disulfide formation is independent of the sulfur concentration (Fig. S5). Temperature dependences of the second- and first-order rate constants for both steps were fitted to the Eyring equation (Fig. S6) to give the activation parameters (Table 1). The first-order sulfur concentration dependence of k_{obs} and the large negative value of $\Delta S^{\ddagger}$ suggest that the first step proceeds via the associative sulfide formation similar to that of **1** and **2** (Scheme 2). On the other hand, from the fact that k_{obs} for the second step is independent of the sulfur concentration giving the large negative value of $\Delta S^{\ddagger}$, the rate-determining step for the disulfide formation is assumed to be associative intramolecular substitution of the coordinated phosphino group for the pendant phosphine sulfide group on palladium(II) followed by the sulfide formation of the dissociated phosphino group (Scheme 2).

3.2. Bridging reaction

Previously, we reported the quantitative formation reactions of the Pd(II)–Pt(II)–Pd(II) and Ni(II)–Pt(II)–Ni(II) trinuclear and Rh(III)–Pd(II)–Pt(II)–Pd(II)–Rh(III) pentanuclear complexes by the stepwise phosphine-bridging reactions of **1**, **3**, and **6** [9]. From the present kinetic results, such a success of the quantitative preparation can be attributed to the existence of the intermediates with a dissociated phosphino group of the bound pp_3 ligand. Because the second steps of the sulfide formation and the phosphine-bridging reaction of the pp_3 complexes correspond to the reactions for the square-planar complexes with the linear tridentate p_3 ligand, the phosphine-bridging reactions of the p_3 complex **4** was compared with those of **1**.

Reaction of **1** with *trans*-$[PtCl_2(NCC_6H_5)_2]$

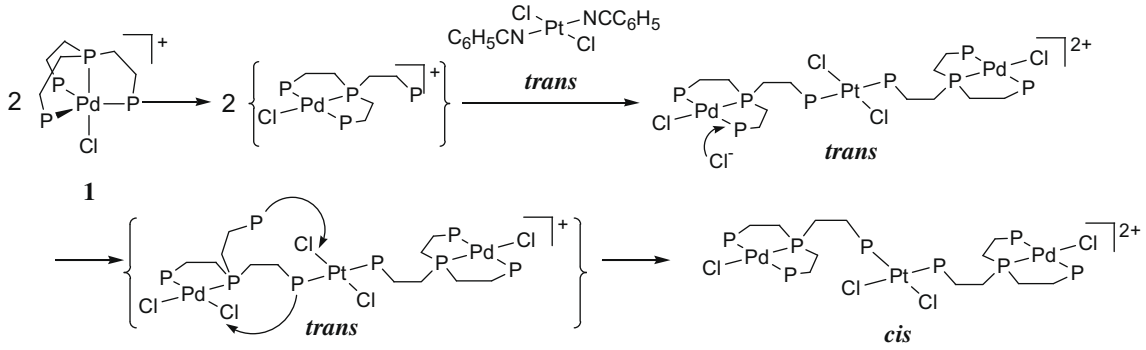

Reaction of **1** with *cis*-$[PtCl_2(NCC_6H_5)_2]$

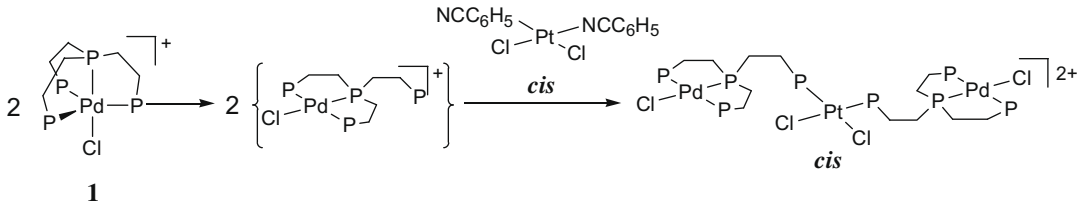

Reaction of **4** with *cis*-$[PtCl_2(NCC_6H_5)_2]$

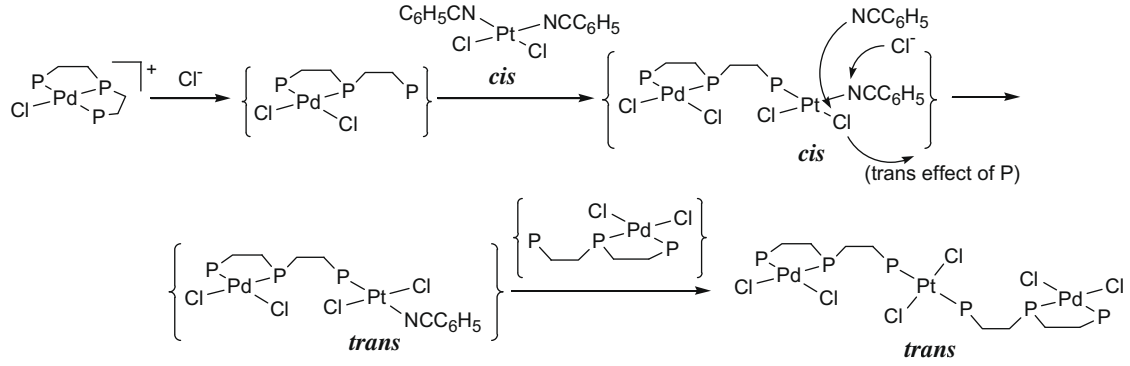

Scheme 3.

The trinuclear structure with a Pd(II)–Pt(II)–Pd(II) metal ion sequence was confirmed by an X-ray analysis of a crystal obtained by the reaction of *cis*-$[PtCl_2(NCPh)_2]$ with 2 equiv. of **4** (Fig. 5). The crystal structure revealed that the *cis* geometry of the starting Pt(II) complex was converted to the *trans* one by the bridging reaction, and the racemic isomer with the same chirality of the two central phosphorus atoms was crystallized. The ^{31}P NMR spectrum of the crude product in chloroform showed two sets of the signals for the Pd(II)–Pt(II)–Pd(II) trinuclear complex with the terminal phosphorus atoms coordinated to Pd(II) at 65.1 and 65.3 ppm ($^3J_{P-P}$ = 10 Hz), the central phosphorus atom at 74.4 and 75.6 ppm, and the terminal phosphorus atom bridging to the central Pt(II) at 14.4 and 15.0 ppm, corresponding to the racemic and meso isomers (Fig. 6). Disappearance of the ^{195}Pt satellite signals in the ^{31}P NMR spectrum arises from relaxation of ^{195}Pt via the chemical shift anisotropy mechanism [16]. Since the AA′XX′ spin system is made up of the two chemically equivalent bridging phosphorus atoms (A and A′) and the two central phosphorus atoms (X and X′), the virtual $^2J_{P-P}$ coupling through Pt(II) center should be observed. The ^{31}P NMR spectral simulation [17] for the bridging phosphorus atom actually gave a large $^2J_{P-P}$ value (650 Hz) characteristic of the *trans* geometry (Fig. S7) [9]. Since one set of the signals at the higher field agreed with the signals for the crystallizing racemic isomer, the other set of signals at the lower field was reasonably assigned to the meso isomer.

As reported previously, while the *trans* isomer of the Pd(II)–Pt(II)–Pd(II) trinuclear complex is initially formed by the reaction of *trans*-$[PtCl_2(NCPh)_2]$ with **1**, the *trans*-to-*cis* geometrical conversion on the Pt(II) center proceeds to give the *cis* isomer as a final product (Scheme 3a) [9]. In contrast with the reaction of *cis*-$[PtCl_2(NCPh)_2]$ with **4** above-mentioned, the *cis* isomer was directly formed without the geometrical conversion by the reaction of *cis*-$[PtCl_2(NCPh)_2]$ with **1** (Scheme 3b) [9]. These facts indicate that the *cis* geometry of the Pt(II) center is thermodynamically more stable than the *trans* one due to the "trans influence" of the phosphorus donor atoms. Because the chelate-ring

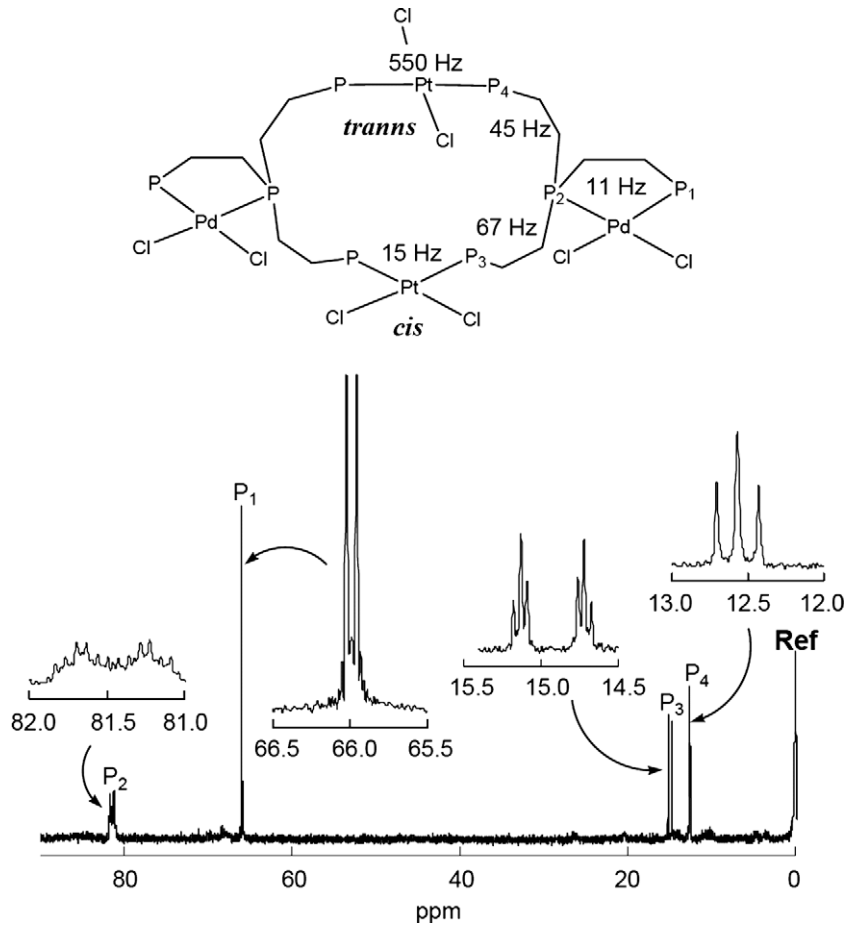

Fig. 7. ^{31}P NMR spectrum of the cyclic tetranuclear complex in chloroform.

opening of the p_3 ligand in **4** is probably very slow and the predissociation equilibrium lies so far to the left compared with the pp_3 ligand in **1**, it is assumed that *cis*-to-*trans* conversion by the "trans effect" of the initially bridging phosphorus atom to the chloro ligand in the *trans* position proceeds prior to the subsequent substitution of benzonitrile for the phosphorus atom in the second bridging step (Scheme 3c). Previously, we proposed the mechanism of the *trans*-to-*cis* conversion of the Pd(II)–Pt(II)–Pd(II) trinuclear complex with the pp_3 ligand, in which the chelate-ring opening of the tridentate-type pp_3 ligand on the Pd(II) terminal moiety by coordination of Cl^- followed by an attack on the Pt(II) center with the dissociated phosphino group are necessary instead of an attack of the Cl^- onto the Pt(II) center (Scheme 3a). This mechanism was confirmed by the fact that the *trans*-to-*cis* conversion of the trinuclear complex with the p_3 ligand, which acts as bidentate on the terminal Pd(II), does not proceeds even though Bu_4NCl was added to provide excess Cl^-. This is consistent with the fact that the further bridging reaction of the bidentate-type phosphine moiety of pp_3 in the Rh(III)–Pd(II)–Pt(II)–Pd(II)–Rh(III) pentanuclear complex does not proceed [9], and the two terminal phosphine chalcogenide groups are selectively formed on $[PdCl(pp_3)]Cl$ by the reaction with excess sulfur or selenium [8].

In the present work, we carried out the reaction of the *cis*-Pd(II)–Pt(II)–Pd(II) trinuclear complex bridged by the pp_3 ligand with 1 equiv. of *cis*-$[PtCl_2(NCPh)_2]$ in chloroform for comparison with the bridging reaction to form the Rh(III)–Pd(II)–Pt(II)–Pd(II)–Rh(III) pentanuclear complex [9]. As shown in Fig. 7, the reaction solution showed the ^{31}P NMR signal of the *trans*-Pt(II) moiety at 12.6 ppm ($^2J_{P-Pt}$ = 550 Hz and $^3J_{P-P}$ = 45 Hz) besides the signal for the originally observed *cis*-Pt(II) central moiety at 14.9 ppm ($^2J_{P-Pt}$ = 15 Hz and $^3J_{P-P}$ = 67 Hz), where the $^2J_{P-Pt}$ and $^3J_{P-P}$ values were obtained by the spectral simulation (Fig. S8) [17]. Furthermore, the two sets of signals for the racemic and meso isomers was changed to one set with the symmetric central phosphorus atoms, showing the signals for the terminal and central phosphino groups coordinated to the Pd(II) terminals at 66.0 ($^3J_{P-P}$ = 11 Hz) and 81.5 ppm, respectively (Fig. 7). This spectrum indicates formation of the cyclic tetranuclear complex with the *cis*- and *trans*-Pt(II) bridges (Scheme 4). Broadening of the ^{195}Pt satellite signals in the ^{31}P NMR spectrum arises from relaxation of ^{195}Pt via the chemical shift anisotropy mechanism [16]. The *cis*-to-*trans* conversion of *cis*-$[PtCl_2(NCPh)_2]$ accompanied by the second bridging step is consistent with the mechanism of the *cis*-to-*trans* conversion for the p_3 bridged trinuclear complex. Interestingly, the *trans*–*cis* bridging structure in the cyclic tetranuclear complex was further converted to the *trans*–*trans* bridging structure (Scheme 4). Such a subsequent steric conversion may be attributable to steric instability of the *trans*–*cis* and *cis*–*cis* bridging structures. The subsequent steric conversion was not observed by the similar reaction of the corresponding Pt(II) complex **5** instead of **1** with *cis*-$[PtCl_2(NCPh)_2]$ to give the *trans*–*cis* tetranuclear complex as a final product, and use of the corresponding Ni(II) complex **6** gave the *trans*–*trans* tetranuclear complex directly. This difference in reactivity depends on the inertness of the metal ions in $[MCl(pp_3)]Cl$ (M = Pd(II) (**1**), Pt(II) (**5**), Ni(II) (**6**)).

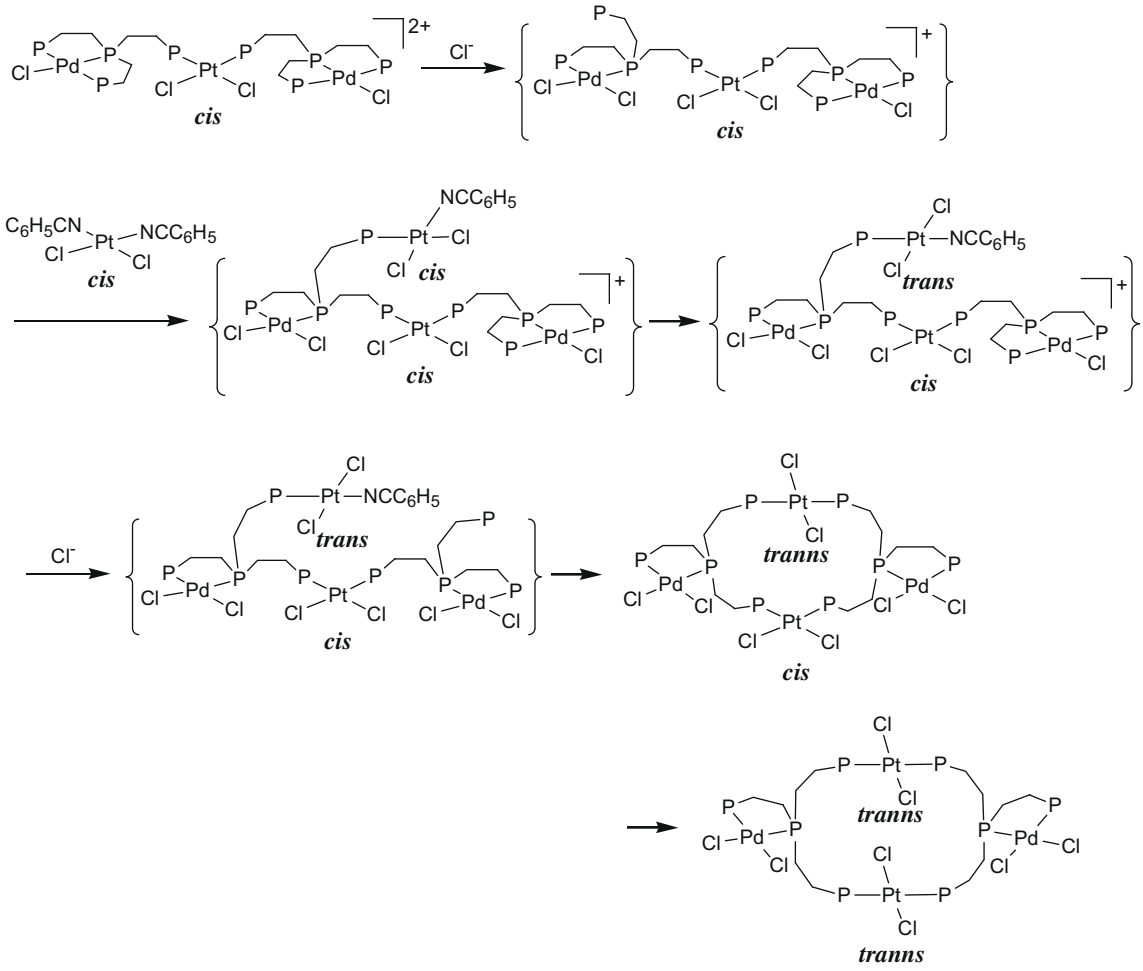

Scheme 4.

Appendix A. Supplementary material

CCDC 755765 contains the supplementary crystallographic data for the trinuclear complex *trans*-[$PtCl_2\{PtCl_2(P_3)\}_2$]. These data can be obtained free of charge from The Cambridge Crystallographic Data Centre via http://www.ccdc.cam.ac.uk/data_request/cif.

Supplementary data associated with this article can be found, in the online version, at doi:10.1016/j.jorganchem.2010.02.006.

References

[1] T.Y.H. Wong, S.J. Rettig, B.R. Jamws, Inorg. Chem. 38 (1999) 2143.
[2] H. Liu, N.A.G. Bandeira, M.J. Calhorda, M.G.B. Drew, J. Félix, V. Novosad, F.F. de Biani, P. Zanwllo, J. Organomet. Chem. 689 (2004) 2808.
[3] N. Zúñiga-Villarreal, J.M. Germán-Acacio, A.A. Lemus-Santana, M. Reyes-Lezama, R.A. Toscano, J. Organomet. Chem. 689 (2004) 2827.
[4] A.N. Skvortsov, A.N. Reznikov, D.A. de Vekki, A.I. Stash, V.K. Belsky, V.N. Spevak, N.K. Skvortsov, Inorg. Chim. Acta 359 (2006) 1031.
[5] D.K. Dutta, P. Chutia, J.D. Woollins, A.M.Z. Slawin, Inorg. Chim. Acta 359 (2006) 877.
[6] P. Sekar, J.A. Ibers, Inorg. Chim. Acta 359 (2006) 2751.
[7] S. Aizawa, A. Majumder, Y. Yokoyama, M. Tamai, O. Maeda, A. Aitamura, Organometallics 28 (2009) 6067.
[8] S. Aizawa, T. Hase, T. Wada, J. Organomet. Chem. 692 (2007) 813.
[9] S. Aizawa, K. Saito, T. Kawamoto, E. Matsumoto, Inorg. Chem. 45 (2006) 4859.
[10] S. Aizawa, T. Iida, S. Funahashi, Inorg. Chem. 35 (1996) 5163.
[11] S. Aizawa, T. Kawamoto, K. Saito, Inorg. Chim. Acta 357 (2004) 2191.
[12] S. Aizawa, T. Kobayashi, T. Kawamoto, Inorg. Chim. Acta 358 (2005) 2319.
[13] G.M. Sheldrick, SHELXS97, Program for Crystal Structure Solution, University of Göttingen, Germany, 1997.
[14] G.M. Sheldrick, SHELXL97, Program for Crystal Structure Refinement, University of Göttingen, Germany, 1997.
[15] J.A. Dobado, H. Martínez-García, J.M. Molina, M.R. Sundberg, J. Am. Chem. Soc. 120 (1998) 8461.
[16] I.M. Ismail, S.J.S. Kerrison, P.J. Sadler, Polyhedron 1 (1982) 57.
[17] *g NMR*, Version 5.0; Adept Scientific plc: Herts, UK.